Journal of Medicinal Chemistry

Article

pubs.acs.org/jmc

Application of the Bicyclo[1.1.1]pentane Motif as a Nonclassical Phenyl Ring Bioisostere in the Design of a Potent and Orally Active γ-Secretase Inhibitor

Antonia F. Stepan,* Chakrapani Subramanyam, Ivan V. Efremov, Jason K. Dutra, Theresa J. O'Sullivan, Kenneth J. DiRico, W. Scott McDonald, Annie Won, Peter H. Dorff, Charles E. Nolan, Stacey L. Becker, Leslie R. Pustilnik, David R. Riddell, Gregory W. Kauffman, Bethany L. Kormos, Liming Zhang, Yasong Lu, Steven H. Capetta, Michael E. Green, Kapil Karki, Evelyn Sibley, Kevin P. Atchison, Andrew J. Hallgren, Christine E. Oborski, Ashley E. Robshaw, Blossom Sneed, and Christopher J. O'Donnell

Pfizer Worldwide Research & Development, Eastern Point Road, Groton, Connecticut 06340, United States

Supporting Information

ABSTRACT: Replacement of the central, para-substituted fluorophenyl ring in the γ-secretase inhibitor **1** (BMS-708,163) with the bicyclo[1.1.1]pentane motif led to the discovery of compound **3**, an equipotent enzyme inhibitor with significant improvements in passive permeability and aqueous solubility. The modified biopharmaceutical properties of **3** translated into excellent oral absorption characteristics (~4-fold ↑ C_{max} and AUC values relative to **1**) in a mouse model of γ-secretase inhibition. In addition, SAR studies into other fluorophenyl replacements indicate the intrinsic advantages of the bicyclo[1.1.1]pentane moiety over conventional phenyl ring replacements with respect to achieving an optimal balance of properties (e.g., γ-secretase inhibition, aqueous solubility/permeability, in vitro metabolic stability). Overall, this work enhances the scope of the [1.1.1]-bicycle beyond that of a mere "spacer" unit and presents a compelling case for its broader application as a phenyl group replacement in scenarios where the aromatic ring count impacts physicochemical parameters and overall drug-likeness.

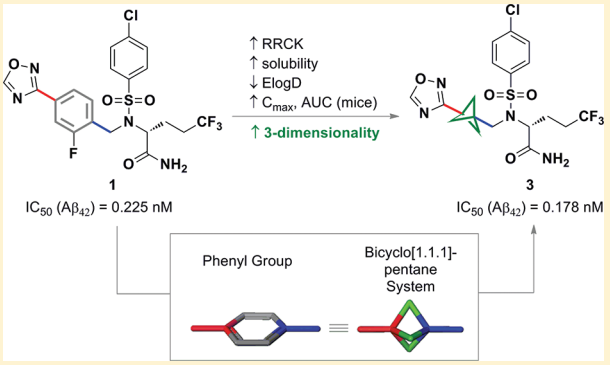

INTRODUCTION

Alzheimer's disease (AD) is the most common cause of dementia in the elderly, with a prevalence of 5% after 65 years of age, increasing to about 30% in people aged 85 years or older. It is characterized clinically by progressive cognitive impairment, often accompanied, in later stages, by psychobehavioral disturbances as well as language impairment.[1] Although the cause of AD is not known, genetic and experimental evidence suggests that β-amyloid peptide (Aβ) chains of 40−42 amino acids are plausible contributors to the pathogenesis of the disease.[2] The APP (β-amyloid precursor protein) is found in many types of cell membranes, and the action of secretases (β and γ) on this precursor protein releases the β-amyloids into the plasma and the cerebrospinal fluid.[3] Subsequent aggregation of these peptides to oligomers and plaques are believed to be the key event in disease progression. γ-Secretase represents a potentially attractive drug target because the enzyme dictates the solubility of the generated Aβ fragment by creating peptides of various lengths, ranging from 37 ($A\beta_{37}$) to 42 ($A\beta_{42}$) amino acid residues.[4] γ-Secretase catabolizes several endogenous substrates, including the Notch signaling protein, which is involved in differentiation and proliferation of embryonic cells, T-cells, and splenic B-cells.[5] Consequently, achieving APP selectivity over Notch signaling protein has become an overarching goal in the design of γ-secretase inhibitors (GSIs), and new inhibitor classes have been shown to selectively lower Aβ production without modulating Notch signaling. Some of these agents, such as **1** (BMS-708,163, Figure 1), have progressed into advanced clinical trials.[6,7]

As part of our efforts to identify novel chemotypes,[8] we have recently reported our structure−activity relationship (SAR) findings on a series of *N*-substituted arylsulfonamides, which culminated in the novel oxetane derivative **2** (Figure 1), a GSI with Notch-sparing activity.[9] To further improve upon the potency of **2** (IC_{50} ($A\beta_{42}$) = 16.9 nM), we explored nonclassical bioisosteric replacements of the central fluorophenyl ring in **1**, which resulted in the identification of compound **3** (Figure 1), a bicyclo[1.1.1]-pentane derivative with subnanomolar γ-secretase inhibitory potency in vitro and a robust pharmacological response in vivo.

Received: January 20, 2012
Published: March 15, 2012

   dx.doi.org/10.1021/jm300094u | *J. Med. Chem.* 2012, 55, 3414−3424

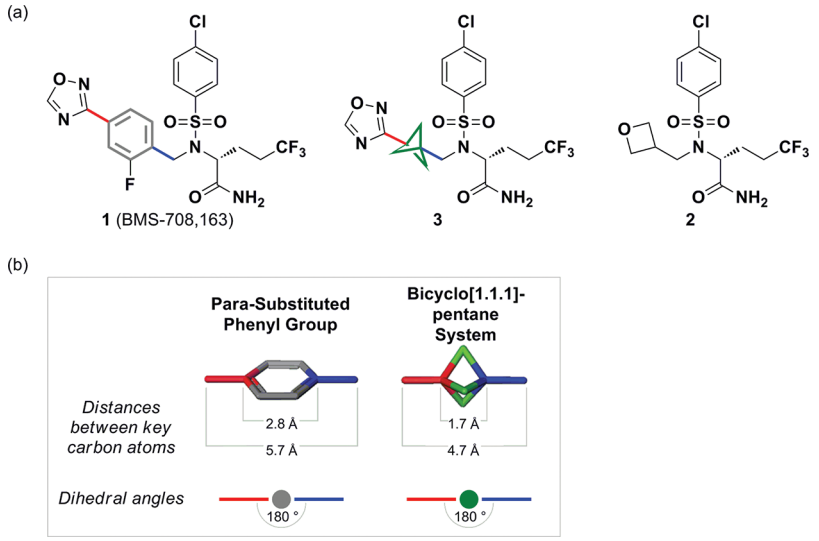

Figure 1. Structures of **1**, its corresponding bicyclo[1.1.1]pentane analogue **3**, and the oxetane-containing GSI **2** (a) and comparison of spacial features between a para-substituted phenyl ring and a disubstituted bicyclo[1.1.1]pentane system (b).

An additional finding resulting from this work is the significant changes in physicochemical attributes upon introduction of the bicyclo[1.1.1]pentane unit, most notably manifested by significant improvements in passive permeability and aqueous solubility relative to **1**. As such, our work provides a compelling case for applications of this bicyclo[1.1.1]pentane system in drug discovery as a strategy to "escape the flatland" imposed by aryl systems[10] and alter the overall physicochemical characteristics during lead optimization.

RESULTS AND DISCUSSION

Chemistry. The synthesis of analogue **3** commenced with the preparation of known nitrile-ester **4** (Scheme 1)[11,12] using a slightly modified literature procedure (see Supporting Information for details). Chemoselective reduction of the ester moiety in **4** with lithium borohydride (THF, 0 → 23 °C) furnished cyanoalcohol **5**, which was coupled to known sulfonamide **6**[7,13] under Mitsunobu conditions to provide **7** (vide infra). Nitrile **7** was converted to the title oxadiazole **3** via a two-step sequence involving treatment with hydroxylamine to generate an intermediate amide-oxime, which was then transformed to **3** in the presence of triethyl orthoformate and a catalytic amount of boron trifluoride etherate.

Scheme 1. Synthesis of Bicyclo[1.1.1]pentane Analogue 3[a]

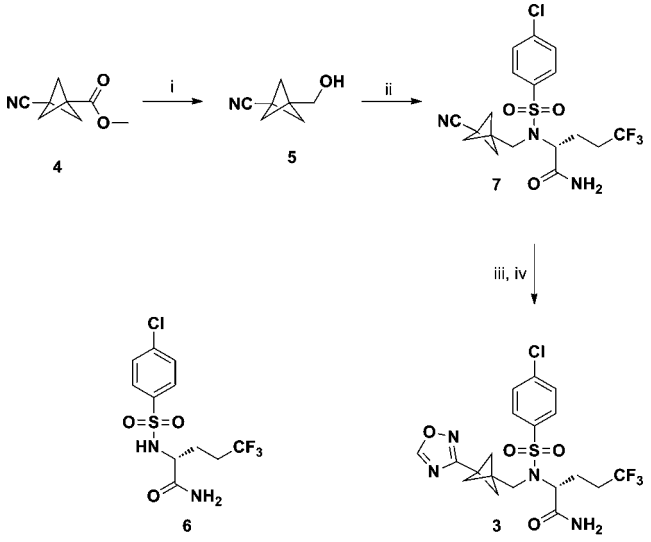

[a]Reagents and conditions: (i) $LiBH_4$, THF, 0 → 23 °C, 18 h (98% yield); (ii) **6**, DIAD, PPh_3, THF, 0 → 23 °C, 18 h (50% yield); (iii) NH_2OH/H_2O (1/1), EtOH, reflux, 3 h; (iv) $BF_3{\cdot}Et_2O$, $CH(OMe)_3$, $(CHCl_2)_2$, 70 °C, 9 h (42% yield over two steps).

The synthesis of analogues **8**–**25** (vide infra) is outlined in Scheme 2 and relied on standard alkylation reactions using either alkyl halides or alcohols. In some cases, the alkylation products were obtained as a diastereomeric mixture, which was separated chromatographically to afford the individual stereoisomers. The desired oxadiazoles were accessed via a two-step protocol involving addition of hydroxylamine to the corresponding nitriles, followed by treatment with triethyl orthoformate and boron trifluoride etherate. Alcohol **26** was accessed from nitrile **27** through α-methylation with methyl iodide in the presence of LDA, followed by hydroboration with 9-BBN (Scheme 3).

Comparison of the in Vitro Pharmacology and Biopharmaceutical Properties of 1 and 3. The rationale for the use of the disubstituted bicyclo[1.1.1]pentane motif as a bioisostere for the central fluorophenyl ring in compound **1** derived from the commonalities in generic spatial features of a para-substituted phenyl ring and a di-substituted bicyclo[1.1.1]-pentane system, which include comparable dihedral angles and similar distances between substituents ("distances between key carbon atoms", Figure 1). This draws parallel with the previous report by Pellicciari et al., who utilized this unusual motif as a phenyl group replacement in the design of a glutamate receptor antagonist.[11] Consistent with this hypothesis, the bicyclo[1.1.1]-pentane analogue **3** exhibited similar degree of γ-secretase inhibition (IC_{50} ($A\beta_{42}$) = 0.178 nM, Table 1) in our whole cell assay when compared with **1** (IC_{50} ($A\beta_{42}$) = 0.225 nM). Under our experimental conditions, the γ-secretase inhibitory potency and Notch selectivity for **1** were comparable to the previously published values.[7] As the stereoelectronic characteristics of the bicyclo[1.1.1]pentane moiety are different from those of a phenyl ring,[11] the similarity in γ-secretase inhibitory potencies of **1** and **3** suggests that the main role of the fluorophenyl group in **1** is that of a spacer and that the bicyclo[1.1.1]pentane

dx.doi.org/10.1021/jm300094u | J. Med. Chem. 2012, 55, 3414–3424

Scheme 2. Synthesis of Compounds 8–25[a]

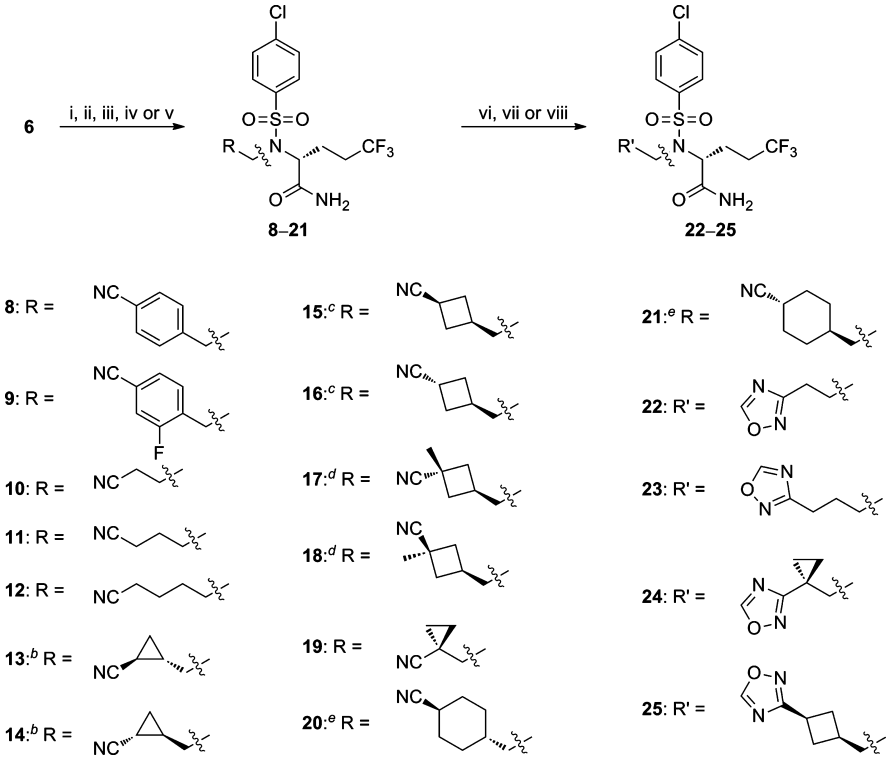

[a]Reagents and conditions: (i) alkyl bromide, TBAI, Cs_2CO_3, DMF, 23 °C; (ii) alkyl bromide, TBAB, K_2CO_3, EtOAc/H_2O (5/1), 50 °C; (iii) alkyl bromide, Cs_2CO_3, DMF, 80 °C, 23–48% yield; (iv) alkyl alcohol, DIAD, PPh_3, THF, 23 °C; (v) alkyl alcohol, DEAD, PPh_3, 23 °C; (vi) (a) NH_2OH·HCl, NEt_3, EtOH, reflux; (b) $(MeO)_3CH$, BF_3·OEt, py, 80 °C; (vii) (a) NH_2OH·HCl, K_2CO_3, EtOH, reflux; (b) $(MeO)_3CH$, BF_3·OEt, THF, 80 °C; (viii) (a) aq NH_2OH, EtOH, 80 °C; (b) $(MeO)_3CH$, BF_3·OEt, $(CH_2Cl_2)_2$, 70 °C. [b]The absolute configuration around the cyclopropane ring was randomly assigned. [c]The absolute configuration around the cyclobutane ring was determined using a series of 2-D NMR spectroscopy experiments (COSY, HSQC, NOESY). [d]The absolute configuration around the cyclobutane ring was randomly assigned. [e]The absolute configuration around the cyclohexane ring was randomly assigned.

Scheme 3. Synthesis of Alcohol 26[a]

[a]Reagents and conditions: (i) MeI, LDA, THF, −78 → 23 °C, 16 h, 54% yield; (ii) 9-BBN, sodium borate, THF, −78 → 23 °C, 16 h, 30% yield.

moiety in **3** orients the oxadiazole and the sulfonamide scaffold in the same well-defined, coplanar orientation found in **1**, as evident from the X-ray structures of the two compounds (Figure 2).

Introduction of the bicyclo[1.1.1]pentane moiety also resulted in significant improvements in the aqueous solubility of **3** (Table 1). In contrast to **1** (kinetic and thermodynamic solubility at pH 6.5 aqueous buffer was measured to be 0.60 and 1.70 μM, respectively), **3** was relatively more soluble with measured kinetic and thermodynamic solubilities of 216 and 19.7 μM, respectively, in pH 6.5 aqueous buffer. We attribute this improvement in solubility to the increased 3-dimensionality of the bicyclo[1.1.1]pentane system relative to a phenyl ring, a characteristic that can possibly prevent intermolecular π-stacking. Besides the improvement in aqueous solubility, **3** also demonstrated a considerable increase in intrinsic permeability in the RRCK assay (**1**, P_{app} = 5.52 × 10^{-6} cm/s; **3**, P_{app} = 19.3 × 10^{-6} cm/s)[14] and was not a substrate for multidrug resistant gene (MDR1)-mediated efflux (P_{app} basolateral to apical (BA)/apical to basolateral (AB) ratio ~1.66) in the MDR1/MDCK assay.[14]

Table 1. In Vitro Pharmacology, Biopharmaceutical, and Disposition Attributes of Compounds 1 and 3

	1	3
IC_{50} ($A\beta_{42}$, nM)[a,b]	0.225 (52)	0.178 (4)
Notch selectivity[b]	350 (14)	178 (4)
human hepatocytes $CL_{int,app}$ (μL/min/million cells)[c]	15.0	<3.80
HLM $CL_{int,app}$ (mL/min/kg)[b,d]	<16.2 (4)	<8.17 (2)
RRCK P_{app} (A to B) (10^{-6} cm/s)[e]	5.52	19.3
ElogD[f]	4.70	3.80
kinetic solubility (pH = 6.5, μM)	0.60	216
thermodynamic solubility (pH = 6.5, μM)	1.70	19.7
thermodynamic solubility (pH = 7.4, μM)	0.90	29.4
MDR1/MDCK BA/AB ratio[g]	1.72	1.66

[a]IC_{50} values were obtained in a whole cell assay using hu APP_{wt} cells by measuring $A\beta_{1-42}$ as previously described.[26] [b]Number of repetitions indicated in parentheses. [c]$CL_{int,app}$ refers to total apparent intrinsic clearance obtained from scaling in vitro half-lives in human hepatocytes.[15] [d]$CL_{int,app}$ refers to total intrinsic clearance obtained from scaling in vitro half-lives in human liver microsomes.[15] [e]RRCK cells with low transporter activity were isolated from Madine–Darby canine kidney cells and were used to estimate intrinsic absorptive permeability.[14] [f]ELogD was measured at pH 7.4.[16] [g]MDR1/MDCK assay utilized MDCK cells transfected with the gene that encodes human p-glycoprotein.[14]

dx.doi.org/10.1021/jm300094u | J. Med. Chem. 2012, 55, 3414–3424

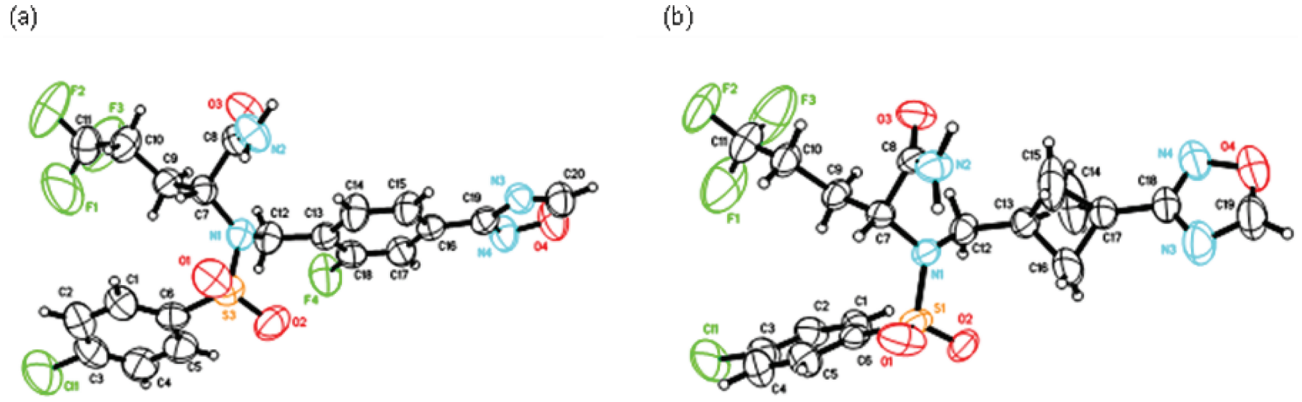

Figure 2. ORTEP representation of the X-ray crystal structures of compounds **1** (a) and **3** (b).

In addition to the altered biopharmaceutical properties, **3** exhibited a greater resistance toward metabolic turnover in cryopreserved human hepatocytes (**3**, apparent intrinsic clearance ($CL_{int,app}$) < 3.8 μL/min/million cells; **1**, $CL_{int,app}$ = 15 μL/min/million cells) and a comparable metabolic stability in human liver microsomes (**3**, HLM $CL_{int,app}$ < 8.17 mL/min/kg; **1**, HLM $CL_{int,app}$ < 16.2 mL/min/kg).[15] The lower $CL_{int,app}$ of **3** (versus **1**) in cryopreserved human hepatocytes is most likely a reflection of its lower lipophilicity (**3**, ELogD = 3.80; **1**, ELogD = 4.70).[16] The ElogD values of **1** and **3** are consistent with the observations correlating lipophilicity reductions with higher degrees of bond saturation (described by parameters such as the aromatic ring count (*N*) and the ratio of sp^3-hybridized carbon atoms to the total carbon count (Fsp^3))[10,17] and translate into clear improvements in lipophilic efficiency (LiPE: **1**, LipE = 4.76; **3**, LipE = 6.55)[18] and the central nervous system multiparameter optimization (CNS MPO: **1**, CNS MPO = 2.49; **3**, CNS MPO = 2.97) desirability score.[19] Furthermore, like **1**, compound **3** was devoid of inhibitory effects on the major human cytochrome P450 (CYP) enzymes.[20] Finally, no other adverse safety risks of compound **3** (relative to **1**) were observed in in vitro safety screens (e.g., dofetilide binding,[21] reactive metabolite assay,[22] and CEREP promiscuity panel).

To further validate the observation that the bicyclo[1.1.1]-pentane system can function as a nonclassical bioisostere for para-substituted phenyl rings within this series of GSIs, the in vitro pharmacologic potency of bicyclo[1.1.1]pentane-containing nitrile analogue **7** was compared to the known phenyl and fluorophenyl derivatives **8**[13a] and **9**.[13b] As shown in Table 2, compound **7** (IC_{50} ($A\beta_{42}$) = 0.99 nM) achieved the same degree of γ-secretase inhibitory potency discerned with the corresponding aryl analogues **8** (IC_{50} ($A\beta_{42}$) = 1.04 nM) and **9** (IC_{50} ($A\beta_{42}$) = 1.77 nM). As noted with compounds **1** and **3**, compound **7** also exhibited an increase in aqueous solubility (**7**, kinetic solubility (pH = 6.5) = 272 μM; **8**, kinetic solubility (pH = 6.5) = 44.5 μM; **9**, kinetic solubility (pH = 6.5) = 6.8 μM) and a decrease in lipophility (**7**, ELogD = 3.80; **8**, ELogD = 4.10; **9**, ELogD = 4.30] relative to **8** and **9**. Passive RRCK permeability and metabolic stability were comparable for all three analogues.

In a parallel series of investigations, the para-substituted aryl rings in compounds **1** and **8** were also replaced with simple alkyl/cycloalkyl spacers to ensure that the bicyclo[1.1.1]pentane system is the optimum replacement for this disubstituted aromatic ring. The resulting compounds **10**–**25** were evaluated for γ-secretase inhibition and in vitro biopharmaceutical properties. As seen in Table 3, none of the compounds **10**–**25** exhibit the appropriate balance between inhibitory potency, metabolic stability, and/or

Table 2. In Vitro Pharmacology and Disposition Data for Compounds 7–9

	8	9	7
IC_{50} ($A\beta_{42}$, nM)[a,b]	1.04 (4)	1.77 (4)	0.99 (4)
Notch selectivity[b]	570 (3)	nd	467 (4)
HLM $CL_{int,app}$ (mL/min/kg)[c]	13.3	<8.00	<8.00
RRCK P_{app} (A to B) (10^{-6} cm/s)[d]	19.7	18.7	30.2
ElogD[e]	4.10	4.30	3.80
MDR1/MDCK BA/AB[f]	2.05	1.71	2.04
kinetic solubility (pH = 6.5, μM)	44.5	6.80	272

[a]IC_{50} values were obtained in a whole cell assay using hu APP_{wt} cells by measuring $A\beta_{1-42}$ as previously described.[21] [b]Number of repetitions indicated in parentheses. [c]$CL_{int,app}$ refers to total intrinsic clearance obtained from scaling in vitro half-lives in human liver microsomes.[15] [d]RRCK cells with low transporter activity were isolated from Madine–Darby canine kidney cells and were used to estimate intrinsic absorptive permeability.[14] [e]ELogD was measured at pH 7.4.[16] [f]MDR1/MDCK assay utilized MDCK cells transfected with the gene that encodes human p-glycoprotein.[14]

passive permeability observed with **3** and **7**. Although limited in scope, these selected examples highlight the advantages of the bicyclo[1.1.1]pentane system over conventional phenyl group replacements[23] with respect to achieving an ideal balance between in vitro inhibitory potency for γ-secretase and disposition properties.

Having established the bicyclo[1.1.1]pentane system as the ideal phenyl replacement, the pharmacokinetic (PK) parameters of **3** were assessed in female rats following intravenous (iv) administration at a dose of 1 mg/kg and oral (po) administration at a dose of 5 mg/kg (Table 4). Female rats were used in this PK assessment due to gender differences in the pharmacokinetic profile of **1** in male versus female rats.[7] Plasma exposure post iv dosing was characterized by a multiexponential elimination. In line with the reported PK for compound **1** in the same species,[7] compound **3** exhibited a low plasma clearance (CL_p) of 13.3 ± 0.35 mL/min/kg, a moderate volume of distibution (V_{ss} = 2.12 ± 0.30 L/kg) and complete oral absorption resulting in an oral bioavailibity of ~100%. Compound **3** also demonstrated sufficient brain partitioning as indicated by its total brain to total plasma (B/P) ratio of 0.61 and its brain availability (BA, calculated as ($f_{u,brain}$[brain])/($f_{u,plasma}$[plasma]) of 0.34.

in Vivo Pharmacology Studies on Compounds 1 and 3. Because of its favorable disposition parameters upon po administration, we next examined whether the good in vitro potency of **3** translated into a robust pharmacodynamic (PD)

dx.doi.org/10.1021/jm300094u | J. Med. Chem. 2012, 55, 3414–3424

Table 3. In Vitro Pharmacology and Disposition Data for Compounds 10−25

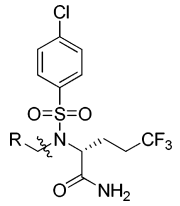

Compound	R	IC_{50} ($A\beta_{42}$, nM)[a,b]	HLM $CL_{int,app}$ (mL/min/kg)[c]	ElogD[d]	RRCK P_{app} (A to B) (10^{-6} cm/s)[e]
10		22.5 (3)	10.5	2.30	10.2
11	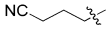	87.1 (4)	14.8	2.55	27.6
12	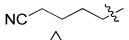	11.1 (5)	21.5	2.70	24.0
13		6.92 (4)	<8.00	2.70	21.5
14		14.7 (4)	<8.00	2.70	9.94
15	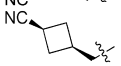	4.77 (4)	62.6	3.20	24.1
16		16.4 (4)	113	2.90	24.9
17		58.7 (3)	<8.00	3.74	21.8
18	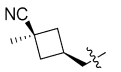	7.47 (3)	<8.00	3.80	25.7
19	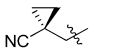	9.60 (4)	14.5	2.65	29.9
20	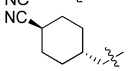	4.11 (3)	31.0	4.00	14.6
21	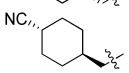	2.75 (3)	>300	4.00	15.7
22	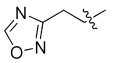	24.4 (3)	18.5	2.50	29.6
23	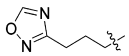	12.1 (5)	112	2.90	31.3
24	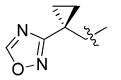	45.5 (3)	36.4	3.70	16.4
25	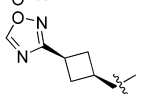	12.3 (3)	156	3.16	14.1

[a] IC_{50} values were obtained in a whole cell assay using hu APP_{wt} cells by measuring $A\beta_{1-42}$ as previously described.[26] [b] Number of repetitions indicated in parentheses. [c] $CL_{int,app}$ refers to total intrinsic clearance obtained from scaling in vitro half-lives in human liver microsomes.[15] [d] ELogD was measured at pH 7.4.[16] [e] RRCK cells with low transporter activity were isolated from Madine−Darby canine kidney cells and were used to estimate intrinsic absorptive permeability.[14]

Table 4. Single-Dose Pharmacokinetic Parameters of Compound 3 in Female Rats[a]

route	dose (mg/kg)	C_{max} (μM)	T_{max} (h)	AUC (0−24 h) (μM·h)	$T_{1/2}$ (h)	CL (mL/min/kg)	V_{ss} (L/kg)	F (%)
iv[b]	1			2.54 ± 0.06	2.18 ± 0.32	13.3 ± 0.35	2.12 ± 0.30	100
po[b]	5	1.86 ± 0.09	2.00 ± 0.00	19.4 ± 0.46				

[a] Data represent means ± standard errors of the mean (n = 3). [b] Vehicle for both iv (2 mL/kg, 0.5 mg/mL) and po (10 mL/kg, 0.5 mg/mL) studies was 40% (w/v) hydroxypropyl-β-cyclodextrin.

response in vivo. Compound **1** was also included as a positive control.[7] Following po administration of compound **3** at 10 and 30 mg/kg and of compound **1** at 30 mg/kg to wild-type male 129/sve mice,[9,24] Aβ lowering was measured in brain, cerebrospinal fluid (CSF), and plasma over a time course of 0−30 and 0−18 h, respectively. The corresponding exposures were also measured in these matrixes to gain an understanding of the PK/PD relationship for γ-secretase inhibition. From a PK perspective, it is noteworthy to comment on the increases in plasma, brain, and CSF concentration of **3** (versus **1**) at the identical 30 mg/kg doses (Table 5, the individual exposure and Aβ values can be found in the Supporting Information), which is most likely a reflection of the improvements in passive permeability and solubility of the [1.1.1] analogue.

From a PD perspective (Figure 3), a significant reduction of Aβ levels relative to the vehicle treated animals was discerned with compound **3** in all three compartments and at both doses. For example, maximum $A\beta_{40}$ and $A\beta_{42}$ reductions in brain were

dx.doi.org/10.1021/jm300094u | J. Med. Chem. 2012, 55, 3414−3424

Table 5. Single-Dose Pharmacokinetic Parameters of Compounds 1 and 3 in 129/sve Mice Following 30 mg/kg po Dosing[a]

compd	C_{max} (μM),[b] plasma	T_{max} (h), plasma	AUC (0–last) (μM·h),[c] plasma	C_{max} (μM),[b] brain	T_{max} (h), brain	AUC (0–last) (μM·h),[c] brain	B/P[d]	BA[e]	C_{max} (μM),[b] CSF	T_{max} (h), CSF	AUC (0–last) (μM·h),[c] CSF
1	1.41 ± 0.24	1	3.63	2.08 ± 0.45	1	5.18	1.43	0.72	0.012 ± 0.002	1	0.024
3	6.48 ± 1.42	1	14.3	5.60 ± 1.69	1	12.0	0.84	0.62	0.053 ± 0.017	1	0.118

[a]Formulation of compound **1** and **3**: 98% (v/v) Phosal 50 PG and 2% Tween (Polysorbate 80). [b]Data represent means ± standard deviations of the mean (compound **1**, n = 4; compound **3**, n = 5). [c]AUC values based on mean matrix concentrations at each time point because this is a nonserial study (compound **1**, AUC (0–18 h); compound **2**, AUC (0–14 h)]. [d]B/P values calculated as AUC_{brain}/AUC_{plasma}. [e]The brain availability is calculated as $(f_{u,brain}[brain])/(f_{u,plasma}[plasma])$. Compound **1**: $f_{u,brain}$ = 0.005, $f_{u,plasma}$ = 0.01. Compound **3**: $f_{u,brain}$ = 0.026, $f_{u,plasma}$ = 0.0354.

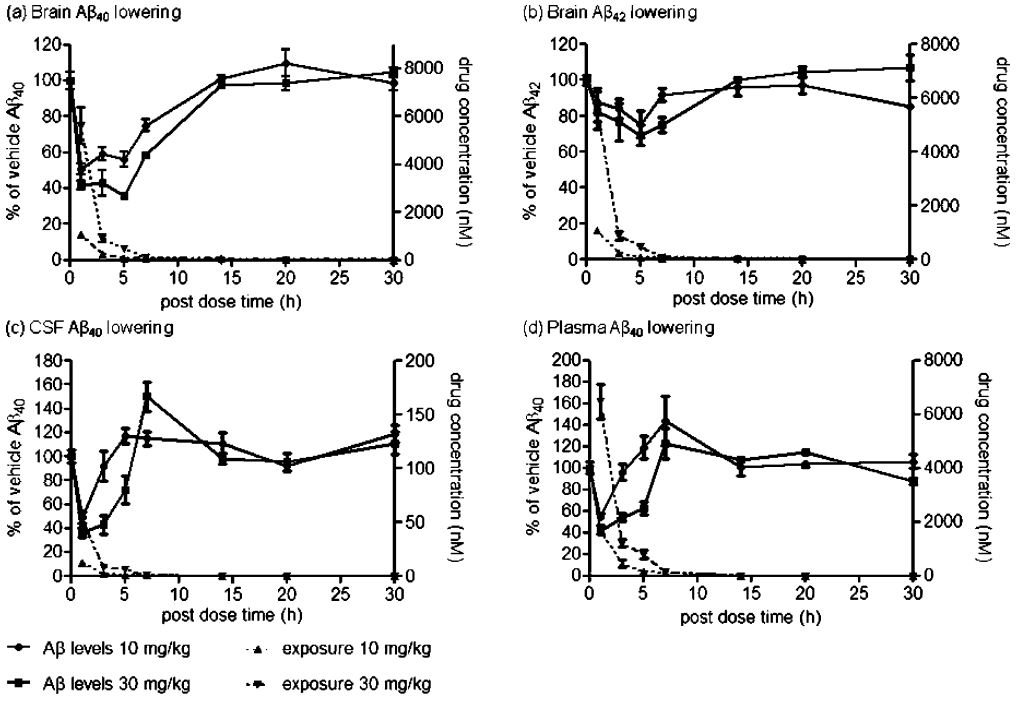

Figure 3. Time course changes of brain Aβ_{40} (a), brain Aβ_{42} (b), CSF Aβ_{40} (c), and plasma Aβ_{40} (d) levels and corresponding exposures (total) of compound **3** following a single dose in wild-type 129/sve mice. Data shown are the mean and standard error of the mean (SEM) as % of vehicle Aβ levels (n = 5 per time point).

observed at 5 h postdose at 30 mg/kg (Figure 3a,b: Aβ_{40} reduction, 64%; Aβ_{42} reduction, 31%). In CSF and plasma (Figure 3c,d), the maximum reductions of Aβ_{40} were 64% and 59%, respectively, and were observed at the 1 h time point post dosing 30 mg/kg. The increase of Aβ_{40} levels at the later time points in both CSF and plasma has been widely observed for multiple GSIs[25] and is probably due to the inhibitor causing an increase in Aβ at low concentrations but inhibition at higher concentrations.[25] The precise mechanisms leading to this rise in Aβ are unknown.[25] At 30 mg/kg, compound **1** demonstrated a comparable PD profile in this preclinical model and induced a maximum reduction of Aβ_{40} and Aβ_{42} in brain at the 4 h time point (Figure 4: Aβ_{40} reduction, 53%; Aβ_{42} reduction, 42%). Maximum reduction in Aβ_{40} levels in CSF (65%) and plasma (55%) were discerned at the 2 and 0.5 h time points, respectively.

CONCLUSION

The identification of compound **3**, an equipotent γ-secretase inhibitor relative to clinical candidate **1**, indicates the fluorophenyl moiety in **1** is not necessarily involved in any enzyme–inhibitor specific interactions and the bicyclo[1.1.1]pentane motif is ideally suited to dispose the oxadiazole and *N*-arylsulfonamide moieties in the required coplanar orientation. A favorable outcome of this exercise was the increase in both passive permeability and aqueous solubility characteristics of **3** relative to **1**, a finding that we attribute to the increased three-dimensionality and concomitant disruption of planarity and intermolecular π-stacking of the two aromatic rings in **1**. These altered physicochemical and biopharmaceutical properties manifested in a significantly improved oral absorption of **3** (relative to **1**) in the mouse model of pharmacology. A such, the attractive in vitro potency, in vivo oral efficacy, and favorable human disposition attributes makes **3** a potential candidate for further preclinical evaluation. Although limited in scope, our SAR studies into alternative replacements of the fluorophenyl group in **1** indicate the superiority of the bicyclo[1.1.1]-pentane functionality over conventional phenyl ring replacements (e.g., alkyl/cycloalkyl spacers) with respect to achieving the desired balance between γ-secretase inhibition, aqueous solubility/permeability, and in vitro metabolic liability. This work therefore highlights the physicochemical changes induced by this unusual phenyl bioisostere and showcases its potential use as a tactic to "escape the flatland" of multiple aryl systems in drug discovery.

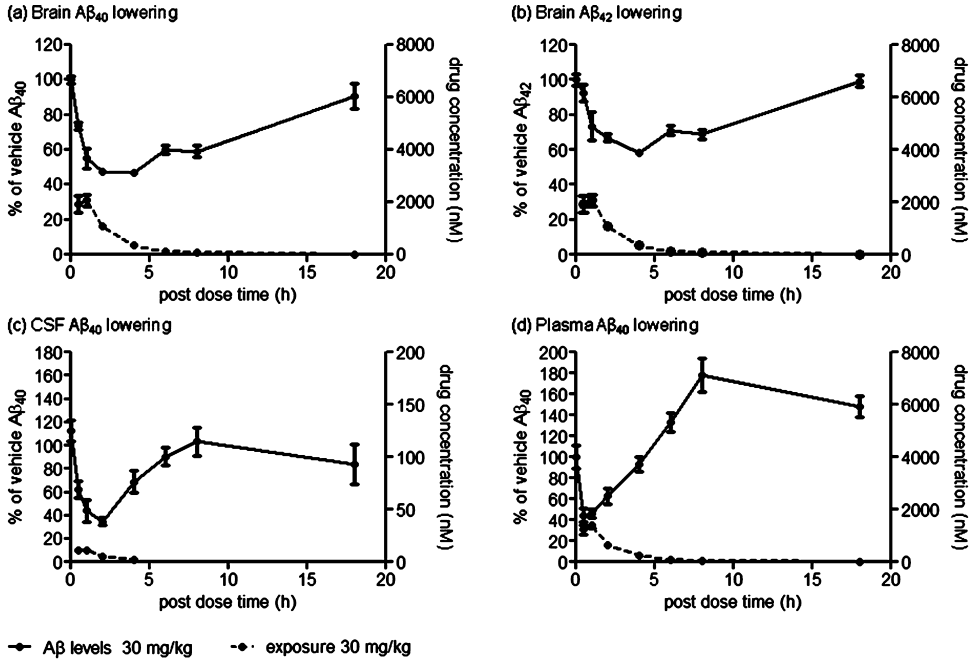

Figure 4. Time course changes of brain Aβ_{40} (a), brain Aβ_{42} (b), CSF Aβ_{40}(c), and plasma Aβ_{40} (d) levels and corresponding exposures (total) of compound **1** levels following a single dose in wild-type 129/sve mice. Data shown are the mean and standard error of the mean (SEM) as % of vehicle Aβ levels (n = 8 per time point).

EXPERIMENTAL SECTION

Chemistry. Unless specified otherwise, starting materials were available from commercial sources. Dry solvents and reagents were of commercial quality and were used as purchased. ^{1}H NMR spectra were recorded on Varian INOVA spectrometers (300, 400, or 500 MHz) (Varian Inc., Palo Alto, CA) at room temperature. Chemical shifts are expressed in parts per million δ relative to residual solvent as an internal reference. Peak multiplicity are expressed as follows: singlet (s), doublet (d), triplet (t), quartet (q), multiplet (m), and broad singlet (br s). The purity of title compounds used in pharmacology testing was verified by HPLC-MS using the following method: 12 min gradient on a HP1100C pump of increasing concentrations of acetonitrile in water (5→95%) containing 0.1% formic acid with a flow rate of 1 mL/min and UV detection at λ 220 and 254 nm on a Gemini C18 150 mm × 4.6 mm, 5 μm column (Phenomenex, Torrance, CA). Title compounds used in pharmacology testing were >95% pure. Electrospray ionization mass spectra were obtained on a Waters ZQ and ZMD instrument (Milford, MA) mass spectrometer operated in positive or negative ionization mode using nitrogen as a carrier gas. Gas chromatography−mass spectroscopy (GC/MS) was performed on a HP 5988A instrument (Palo Alto, CA). All synthetic reactions were carried out under nitrogen atmosphere or in sealed vials. The chemical yields reported below are unoptimized specific examples of one preparation.

*3-(Hydroxymethyl)bicyclo[1.1.1]pentane-1-carbonitrile (**5**).* To a solution of **4** (190 mg, 1.26 mmol) in tetrahydrofuran (6.0 mL) at 0 °C was added lithium borohydride (2.0 M in tetrahydrofuran, 630 μL, 1.26 mmol). The reaction mixture was stirred at 23 °C for 12 h. The cloudy mixture was then cooled to 0 °C (external), and methanol (12 mL) was added dropwise. This mixture was stirred at 23 °C for 2 h, and the solvent was removed in vacuo. The crude product was purified by flash column chromatography using a 0→100% gradient of ethyl acetate/heptane to afford 166 mg (100% yield) of **5** as a colorless oil. ^{1}H NMR (500 MHz, $CDCl_3$) δ 3.62 (d, J = 5.61 Hz, 2H), 2.21 (s, 6H), 1.32 (t, J = 5.74 Hz, 1H). GCMS m/z 122 (M − H$^+$).

*(R)-2-{4-Chloro-N-[(3-cyanobicyclo[1.1.1]pentan-1-yl)methyl]-phenylsulfonamide-5,5,5-trifluoropentanamide (**7**).* To a solution of **6** (552 mg, 1.60 mmol) and **5** (197 mg, 1.60 mmol) in tetrahydrofuran (8.0 mL) at 0 °C was added triphenylphosphine (639 mg, 2.40 mmol). Diisopropyl azodicarboxylate (470 μL, 2.40 mmol) was then added dropwise, and the reaction mixture was stirred at 23 °C for 12 h. The reaction mixture was loaded directly onto a silica gel cartridge and was purified by flash column chromatography using a 0→75% gradient of ethyl acetate/heptane to afford 460 mg (64% yield) of **7** as a white solid. ^{1}H NMR (500 MHz, $CDCl_3$) δ 7.78−7.70 (m, 2H), 7.60−7.51 (m, 2H), 6.48 (br s, 1H), 5.44 (br s, 1H), 4.15 (dd, J = 9.76, 5.13 Hz, 1H), 3.41 (d, J = 16.1 Hz, 1H), 3.24 (d, J = 16.1 Hz, 1H), 2.27−2.18 (m, 6H), 2.17−2.06 (m, 1H), 2.01−1.89 (m, 1H), 1.82−1.69 (m, 1H), 1.24−1.11 (m, 1H). ^{13}C NMR (125 MHz, $CDCl_3$) δ 170.5, 140.5, 137.2, 129.9 (2 C), 128.4 (2 C), 126.3 (q, J = 276.1 Hz), 117.4, 57.72, 54.50 (3 C), 44.91, 42.99, 30.34 (q, J = 29.5 Hz), 23.29, 20.86 (q, J = 2.80 Hz). LCMS m/z 450 (M + H$^+$); $[\alpha]_D^{24}$ = +9.80° (c 1.1, $CHCl_3$).

*(R)-2-{N-{[3-(1,2,4-Oxadiazol-3-yl)bicyclo[1.1.1]pentan-1-yl]-methyl}-4-chlorophenylsulfonamido}-5,5,5-trifluoropentanamide (**3**).* To a solution of 7 (1.35 g, 3.00 mmol) in ethanol (30 mL) was added hydroxylamine (50 wt % in water, 793 mg, 12.0 mmol). The resulting reaction mixture was heated at 80 °C for 90 min and then cooled to 23 °C and concentrated in vacuo. Dichloromethane (250 mL) and water (60 mL) were added, the phases were separated, and the organic layer was washed with brine, dried (Na_2SO_4), filtered, and concentrated in vacuo to afford the intermediate amide-oxime as an off-white solid, which was used in the next step without further purification. To a mixture of the crude amide-oxime (1.39 g, 2.88 mmol) and trimethyl orthoformate (920 mg, 8.67 mmol) in 1,2-dichloroethane (30 mL) was added boron trifluoride diethyl etherate (62.1 mg, 0.15 mmol) at 23 °C. The resulting mixture was stirred at 80 °C under a water-cooled reflux condenser for 10 h, cooled to 23 °C, dry-loaded, and then purified by flash column chromatography using a 0→70% gradient of ethyl acetate/heptane to afford 618 mg (42% yield) of **3** as a white solid; mp = 163−165 °C (recrystallized from a mixture of ethyl acetate and heptane). ^{1}H NMR (500 MHz, $CDCl_3$) 8.64 (s, 1H), 7.83−7.78 (m, 2H), 7.60−7.51 (m, 2H), 6.62 (br s, 1H), 5.53 (br s, 1H), 4.18 (dd, J = 9.52, 5.61 Hz, 1H), 3.45 (q, J = 15.9 Hz, 2H), 2.27−2.13 (m, 7H), 2.02−1.89 (m, 1H), 1.89−1.74 (m, 1H), 1.35−1.26 (m, 1H). ^{13}C NMR (125 MHz, $CDCl_3$) δ 170.5, 167.2, 164.7, 140.4, 137.5, 129.9, 128.6, 126.4 (q, J = 275.0 Hz), 58.1, 52.8, 45.8, 40.8, 32.9, 30.5 (q, J = 28.8 Hz), 21.1 (q, J = 2.5 Hz). LCMS m/z 493 (M + H$^+$); $[\alpha]^{24}_D$ +13.2° (c 0.78, $CHCl_3$).

dx.doi.org/10.1021/jm300094u | J. Med. Chem. 2012, 55, 3414−3424

*(R)-2-[4-Chloro-N-(4-cyanobenzyl)phenylsulfonamido]-5,5,5-trifluoropentanamide (**8**).* To a solution of **6** (34.0 mg, 0.10 mmol) in dimethylformamide (172 μL) at 23 °C was added 4-(bromomethyl)-benzonitrile (19.6 mg, 0.10 mmol), followed by cesium carbonate (103 mg, 0.31 mmol). The reaction mixture was stirred at that temperature for 48 h. Ethyl acetate (2 mL) and water (1 mL) were then added. The biphasic mixture was loaded onto a Varian ChemElut (Hydromatrix) cartridge (6 cm^3, 1 g sorbent). After 5 min, the cartridge was eluted with ethyl acetate (2 × 3 mL) and the solvent was removed. The crude material was dissolved in dimethyl sulfoxide (1 mL) and purified by reversed phase HPLC (Waters XBridge C18 column; mobile phase: 55/45→0/100 gradient of 0.1% NH_4OH in water/0.1% NH_4OH in acetonitrile). Removal of the solvent in vacuo afforded 22.2 mg (48% yield) of **8** as a white foam. ^1H NMR (500 MHz, $CDCl_3$) δ 7.74−7.68 (m, 2H), 7.65−7.60 (m, 2H), 7.57−7.52 (m, 2H), 7.49 (d, *J* = 8.54 Hz, 2H), 6.20 (br s, 1H), 5.25 (br s, 1H), 4.64 (d, *J* = 16.1 Hz, 1H), 4.42 (d, *J* = 15.9 Hz, 1H), 4.36 (dd, *J* = 8.91, 6.22 Hz, 1H), 2.20−2.08 (m, 1H), 2.08−1.93 (m, 1H), 1.88−1.71 (m, 1H), 1.47−1.36 (m, 1H). LCMS *m*/*z* 460 (M + H^+).

*(R)-2-[4-Chloro-N-(4-cyano-2-fluorobenzyl)phenylsulfonamido]-5,5,5-trifluoropentanamide (**9**).* To a solution of **6** (1.18 g, 3.42 mmol) in ethyl acetate (12 mL) and water (2.4 mL) at 23 °C was added 4-(bromomethyl)-3-fluorobenzonitrile (0.73 mg, 3.42 mmol), followed by potassium carbonate (946 mg, 6.85 mmol) and tetrabutylammonium bromide (0.17 mg, 0.51 mmol). The reaction mixture was stirred at 50 °C for 48 h. To the cooled reaction mixture (23 °C), ethyl acetate (100 mL) and water (100 mL) were added. The phases were separated, the organics were washed with water (100 mL) and brine, dried (Na_2SO_4), filtered, and concentrated in vacuo. The crude product was purified by flash column chromatography using a 0→25% gradient of ethyl acetate/dichloromethane to afford 1.26 g (77% yield) of **9** as a white foam. ^1H NMR (500 MHz, $CDCl_3$) δ 7.76−7.71 (m, 2H), 7.68 (t, *J* = 7.69 Hz, 1H), 7.57−7.52 (m, *J* = 8.79 Hz, 2H), 7.46 (d, *J* = 8.05 Hz, 1H), 7.32 (d, *J* = 9.52 Hz, 1H), 6.29 (br s, 1H), 5.35 (br s, 1H), 4.67 (d, *J* = 16.1 Hz, 1H), 4.49 (d, *J* = 16.1 Hz, 1H), 4.39 (dd, *J* = 9.15, 5.98 Hz, 1H), 2.18 (dtd, *J* = 14.2, 8.79, 5.86 Hz, 1H), 2.07−1.93 (m, 1H), 1.90−1.75 (m, 1H), 1.48−1.38 (m, 1H). $[\alpha]^{20}_D$ +33.0° (*c* 1.00, DMSO).

*(R)-2-[4-Chloro-N-(2-cyanoethyl)phenylsulfonamido]-5,5,5-trifluoropentanamide (**10**).* To a solution of **6** (500 mg, 1.45 mmol) in dimethylformamide (2.0 mL) at 23 °C was added 3-bromopropanenitrile (388 mg, 2.90 mmol), followed by cesium carbonate (945 mg, 2.90 mmol). The reaction mixture was stirred at 80 °C for 12 h. The reaction mixture was then filtered through Celite, and the resulting filtrate was concentrated in vacuo. The crude product was purified by flash column chromatography using a 0→7.5% gradient of 7 N methanolic NH_3/dichloromethane to afford 132 mg (22% yield) of **10** as a colorless oil. ^1H NMR (400 MHz, $CDCl_3$) δ 7.83−7.77 (m, 2H) 7.61−7.56 (m, 2H), 6.41 (br s, 1H), 5.51 (br s, 1 H), 4.28 (dd, *J* = 9.39, 6.06 Hz, 1H), 3.68−3.58 (m, 1H), 3.50 (ddd, *J* = 15.1, 8.22, 5.28 Hz, 1H), 2.92−2.73 (m, 2H), 2.24−2.11 (m, 1H), 2.09−1.84 (m, 2H), 1.44 (td, *J* = 14.3, 6.85 Hz, 1H). LCMS *m*/*z* 398 (M + H^+).

*(R)-2-[4-Chloro-N-(3-cyanopropyl)phenylsulfonamido]-5,5,5-trifluoropentanamide (**11**).* To a solution of **6** (300 mg, 0.87 mmol) in dimethylformamide (8 mL) at 23 °C was added 4-bromo-butyronitrile (193 mg, 1.30 mmol) followed by cesium carbonate (511 mg, 1.57 mmol) and tetrabutylammonium iodide (73.8 mg, 0.20 mmol). The reaction mixture was stirred at that temperature for 12 h. Ethyl acetate (20 mL) was then added, and the organic layer was washed with water (10 mL), a saturated solution of sodium bicarbonate (10 mL), and brine (10 mL). The organics were dried ($MgSO_4$), filtered, and concentrated in vacuo. The crude product was purified by flash column chromatography using a 25→50% gradient of ethyl acetate/heptane to afford 192 mg (53% yield) of **11** as a clear gum. ^1H NMR (400 MHz, $CDCl_3$) δ 7.76−7.70 (m, 2H), 7.55−7.50 (m, 2H), 6.44 (br s, 1H), 5.53 (br s, 1H), 4.27 (dd, *J* = 9.18, 6.05 Hz, 1H), 3.50−3.39 (m, 1H), 3.22−3.12 (m, 1H), 2.38 (t, *J* = 7.42 Hz, 2H), 2.22−2.09 (m, 1H), 2.01−1.91 (m, 3H), 1.85−1.71 (m, 1H), 1.32 (dd, *J* = 14.3, 8.20 Hz, 1H). LCMS *m*/*z* 412 (M + H^+).

*(R)-2-[4-Chloro-N-(4-cyanobutyl)phenylsulfonamido]-5,5,5-trifluoropentanamide (**12**).* Compound **6** (400 mg, 1.16 mmol), bromopentanenitrile (282 mg, 1.74 mmol), cesium carbonate (680 mg, 2.10 mmol), and tetrabutylammonium iodide (100 mg, 0.27 mmol) were used to synthesize **12** using the procedure described for the preparation of **11**. The crude product was purified by flash column chromatography using a 25→50% gradient of ethyl acetate/heptane to afford 156 mg (31% yield) of **12** as a clear gum. ^1H NMR (400 MHz, $CDCl_3$) δ 7.73 (d, *J* = 8.00 Hz, 2H), 7.52 (d, *J* = 8.59 Hz, 2H), 6.50 (br s, 1H), 5.47 (br s, 1H), 4.22 (dd, *J* = 9.18, 6.05 Hz, 1H), 3.42−3.31 (m, 1H), 3.19−3.09 (m, 1H), 2.36 (t, *J* = 6.93 Hz, 2H), 2.21−2.08 (m, 1H), 2.03−1.86 (m, 1H), 1.84−1.59 (m, 5H), 1.38−1.25 (m, 1H). LCMS *m*/*z* 426 (M + H^+).

*(R)-2-{4-Chloro-N-{[(1S,2S)-2-cyanocyclopropyl]methyl}-phenylsulfonamido}-5,5,5-trifluoropentanamide (**13**) and (R)-2-{4-Chloro-N-{[(1R,2R)-2-cyanocyclopropyl]methyl}-phenylsulfonamido}-5,5,5-trifluoropentanamide (**14**).* Compound **6** (593 mg, 1.72 mmol), *trans*-2-(hydroxymethyl)cyclopropanecarbonitrile (racemic) (167 mg, 1.72 mmol), triphenylphosphine (729 mg, 2.76 mmol), and diethyl azodicarboxylate (443 μL, 2.41 mmol) were used to synthesize **13** and **14** using the procedure described for the preparation of **7**. The crude product was purified by supercritical fluid chiral chromatography (MiniGram-2 Chiralcel OJ-H column; mobile phase: 90/10 CO_2/MeOH) to afford 10.0 mg (1.4% yield) of **13** as a white solid and 10.0 mg (1.4% yield) of **14** as a white solid. The absolute configuration of both isomers was randomly assigned. **13**: ^1H NMR (400 MHz), $CDCl_3$) δ 7.76−7.72 (m, 2H), 7.58−7.54 (m, 2H), 6.63 (s, 1H), 5.73 (s, 1H), 4.31−4.27 (m, 1H), 3.30 (dd, *J* = 15.4, 5.85 Hz, 1H), 3.12 (dd, *J* = 15.4, 8.78 Hz, 1H), 2.28−2.18 (m, 1H), 2.06−1.92 (m, 1H), 1.90−1.70 (m, 2H), 1.56−1.51 (m, 1H), 1.39−1.30 (m, 2H), 1.09−1.04 (m, 1H); LCMS *m*/*z* 424 (M + H^+). **14**: ^1H NMR (400 MHz, $CDCl_3$) δ 7.80−7.77 (m, 2H), 7.59−7.55 (m, 2H), 6.58 (s, 1H), 5.79 (s, 1H), 4.28 (dd, *J* = 9.17, 6.05 Hz, 1H), 3.43 (dd, *J* = 15.6, 5.66 Hz, 1H), 2.98 (dd, *J* = 15.8, 8.00 Hz, 1H), 2.21−2.12 (m, 1H), 2.06−1.91 (m, 1H), 1.86−1.76 (m, 2H), 1.47−1.42 (m, 1H), 1.34−1.23 (m, 2H), 1.03−0.97 (m, 1H); LCMS *m*/*z* 424 (M + H^+).

*(R)-2-{4-Chloro-N-{[(1S,3S)-3-cyanocyclobutyl]methyl}-phenylsulfonamido}-5,5,5-trifluoropentanamide (**15**) and (R)-2-{4-Chloro-N-{[(1R,3R)-3-cyanocyclobutyl]methyl}phenylsulfonamido}-5,5,5-trifluoropentanamide (**16**).* Compound **6** (300 mg, 0.87 mmol), hydroxymethyl-cyclobutanecarbonitrile (106 mg, 0.96 mmol), triphenylphosphine (280 mg, 1.10 mmol), and diisopropyl azodicarboxylate (280 mg, 1.30 mmol) were used to synthesize **15** and **16** using the procedure described for the preparation of **7**. The crude product was purified by supercritical fluid chiral chromatography (Chiralpak AD-H column; mobile phase: 85/15 CO_2/methanol) to afford 69.0 mg (52% yield) of **15** (*cis*) as a clear glass and 25.0 mg (6.6% yield) of **16** (*trans*) as a clear glass. The relative configuration across the cyclopropane ring was determined using a series of 2D NMR experiments (COSY, HSQC, NOESY). **15**: ^1H NMR (400 MHz, $CDCl_3$) δ 7.72 (d, *J* = 8.59 Hz, 2H), 7.53 (d, *J* = 8.59 Hz, 2H), 6.51 (br s, 1H), 5.48 (br s, 1H), 4.20 (dd, *J* = 9.37, 5.85 Hz, 1H), 3.44 (dd, *J* = 14.64, 8.98 Hz, 1H), 3.07 (dd, *J* = 14.7, 5.56 Hz, 1H), 2.91 (quintet, *J* = 8.98 Hz, 1H), 2.68−2.53 (m, 1H), 2.52−2.37 (m, 2H), 2.29−2.18 (m, 1H), 2.18−1.83 (m, 3H), 1.73 (ddd, *J* = 15.2, 9.90, 5.56 Hz, 1H), 1.33−1.14 (m, 1H); LCMS *m*/*z* 438 (M + H^+). **16**: ^1H NMR (400 MHz, $CDCl_3$) δ 7.70 (d, *J* = 8.59 Hz, 2H), 7.51 (d, *J* = 8.59 Hz, 2H), 6.51 (br s, 1H), 5.72 (br s, 1H), 4.17 (dd, *J* = 9.37, 5.66 Hz, 1H), 3.47 (dd, *J* = 14.6, 9.96 Hz, 1H), 3.15−3.04 (m, 1H), 2.89−2.75 (m, 1H), 2.50−2.34 (m, 2H), 2.34−2.25 (m, 1H), 2.17−1.99 (m, 2H), 1.99−1.85 (m, 1H), 1.78−1.62 (m, 1H), 1.28−1.12 (m, 2H); LCMS *m*/*z* 438 (M + H^+).

*(R)-2-{4-Chloro-N-{[(1R,3R)-3-cyano-3-methylcyclobutyl]methyl}-phenylsulfonamido}-5,5,5-trifluoropentanamide (**17**) and (R)-2-{4-Chloro-N-{[(1S,3S)-3-cyano-3-methylcyclobutyl]methyl}-phenylsulfonamido}-5,5,5-trifluoropentanamide (**18**).* Compound **6** (90.0 mg, 0.26 mmol), 3-(hydroxymethyl)-1-methylcyclobutanecarbonitrile (**26**, 42.4 mg, 0.34 mmol), triphenylphosphine (88.9 mg, 0.34 mmol), and diisopropyl azodicarboxylate (78.5 mg, 0.37 mmol) were used to synthesize **17** and **18** using the procedure described for the preparation of **7**. The crude product was purified by flash column chromatography using a 0→50% gradient of ethyl acetate/heptane.

dx.doi.org/10.1021/jm300094u | *J. Med. Chem.* 2012, 55, 3414−3424

The obtained material was further purified by supercritical fluid chiral chromatography (Chiralpak OD-H column; mobile phase: 90/10 CO_2/methanol) to afford 1.50 mg (1.3% yield) of **17** (*trans*) as a clear glass and 7.10 mg (6.0% yield) of **18** (*cis*, as a 82:12 mixture of **18**:**17**) as a clear glass. The absolute configuration of both isomers was randomly assigned. **17**: ^{1}H NMR (400 MHz, $CDCl_3$) δ 7.72−7.70 (m, 2H), 7.53−7.51 (m, 2H), 6.50 (br s, 1H), 5.41 (br s, 1H), 4.20−4.12 (m, 1H), 3.42−3.31 (m, 1H), 3.17−3.06 (m, 1H), 2.87−2.74 (m, 1H), 2.65−2.52 (m, 2H), 2.20−2.06 (m, 1H), 2.00−1.86 (m, 2H), 1.78−1.65 (m, 2H), 1.46 (s, 3H), 1.27−1.15 (m, 1H). **18**, title compound peaks only: 7.74−7.72 (m, 2H), 7.55−7.52 (m, 2H), 6.51 (br s, 1H), 5.47 (br s, 1H), 4.27−4.19 (m, 1H), 3.57−3.47 (m, 1H), 3.15−3.06 (m, 1H), 2.75−2.63 (m, 1H), 2.50−2.40 (m, 1H), 2.26−2.17 (m, 1H), 2.17−2.06 (m, 3H), 2.05−1.87 (m, 1H), 1.80−1.64 (m, 1H), 1.50 (s, 3H), 1.33−1.18 (m, 1H). Mixture of **17** and **18**: LCMS m/z 452 (M + H$^+$).

*(R)-2-{4-Chloro-N-[(1-cyanocyclopropyl)methyl]-phenylsulfonamido}-5,5,5-trifluoropentanamide (**19**).* Compound **6** (1.00 g, 2.90 mmol), 1-hydroxymethyl-cyclopropanecarbonitrile (366 mg, 3.77 mmol), triphenylphosphine (989 mg, 3.77 mmol), and diisopropyl azodicarboxylate (811 mg, 3.77 mmol) were used to synthesize **19** using the procedure described for the preparation of **7**. The crude product was purified by preparative reversed phase HPLC (Phenomenex Gemini C18 column; mobile phase: 75:25→0:100 gradient of 0.1% NH_4OH in water/0.1% NH_4OH in methanol) to afford 650 mg (52% yield) of **19** as a white solid. ^{1}H NMR (400 MHz, $CDCl_3$) δ 7.86 (dd, J = 8.59, 1.76 Hz, 2H), 7.54 (dd, J = 8.49, 1.66 Hz, 2H), 6.62 (br s, 1H), 5.50 (br s, 1H), 4.28 (dd, J = 8.20, 6.83 Hz, 1H), 3.50 (d, J = 15.4 Hz, 1H), 3.28 (d, J = 15.4 Hz, 1H), 2.28−2.14 (m, 1H), 2.05−1.83 (m, 2H), 1.60−1.48 (m, 1H), 1.31 (s, 2H), 1.15−1.08 (m, 1H), 1.01−0.93 (m, 1H). LCMS m/z 424 (M + H$^+$).

*(R)-2-{4-Chloro-N-{[(1R,4R)-4-cyanocyclohexyl]methyl}-phenylsulfonamido}-5,5,5-trifluoropentanamide (**20**) and (R)-2-{4-Chloro-N-{[(1R,4R)-4-cyanocyclohexyl]methyl}phenylsulfonamido}-5,5,5-trifluoropentanamide (**21**).* Compound **6** (414 mg, 1.20 mmol), 4-(hydroxymethyl)cyclohexanecarbonitrile (mixture of *cis*- and *trans*-isomers) (250 mg, 1.50 mmol), triphenylphosphine (470 mg, 1.88 mmol), and diethyl azodicarboxylate (283 μL, 1.80 mmol) were used to synthesize **20** and **21** using the procedure described for the preparation of **6**. The crude product was purified by supercritical fluid chiral chromatography (MiniGram-1 Chiralpak AS-H column; mobile phase: 85/15 CO_2/ethanol) to afford 10.0 mg (1.8% yield) of **20** as a white solid and 22.0 mg (3.9% yield) of **21** as a white solid. The absolute configuration of both isomers was randomly assigned. **20**: ^{1}H NMR (400 MHz, $CDCl_3$) δ 7.77−7.74 (m, 2H), 7.58−7.55 (m, 2H), 6.69 (s, 1H), 5.44 (s, 1H), 4.26 (dd, J = 9.76, 5.46 Hz, 1H), 3.34 (dd, J = 14.4, 10.2 Hz, 1H), 2.96−2.91 (m, 2H), 2.22−2.12 (m, 1H), 2.08, 1.87 (m, 4H), 1.82−1.58 (m, 4H), 1.52−1.23 (m, 4H); LCMS m/z 466 (M + H$^+$). **21**: ^{1}H NMR (400 MHz, $CDCl_3$) δ 7.73 (d, J = 8.59 Hz, 2H), 7.55 (d, J = 8.59 Hz, 2H), 6.64 (s, 1H), 5.53 (s, 1H), 4.25−4.21 (m, 1H), 3.26−3.20 (m, 1H), 2.94−2.89 (m, 1H), 2.41−1.96 (m, 6H), 1.76−1.47 (m, 6H), 1.02−0.76 (m, 2H); LCMS m/z 466 (M + H$^+$).

*(R)-2-{N-[2-(1,2,4-Oxadiazol-3-yl)ethyl]-4-chlorophenylsulfonamido}-5,5,5- trifluoropentanamide (**22**).* To a solution of **10** (70.0 mg, 0.18 mmol) in ethanol (2.0 mL) at 23 °C was added hydroxylamine (50% v/v in water, 46.5 mg, 0.70 mmol). The reaction mixture was stirred at 80 °C for 1 h. The solvent was then removed in vacuo, and the resulting material was diluted with dichloromethane (5.0 mL) and washed with water (5.0 mL). The organic layer was dried ($MgSO_4$), filtered, and concentrated in vacuo. The crude product was purified by flash column chromatography using a 25 → 50% gradient of ethyl acetate/heptane to afford 72.0 mg (96% yield) of the intermediate amide-oxime as a colorless solid. ^{1}H NMR (400 MHz, MeOD) δ 7.93−7.88 (m, 2H), 7.62−7.57 (m, 2H), 4.39−4.34 (m, 1H), 3.68−3.59 (m, 1 H), 3.48 (ddd, J = 15.2, 9.88, 5.28 Hz, 1H), 2.57−2.39 (m, 2H), 2.18−2.04 (m, 3H), 1.83−1.74 (m, 1 H). LCMS m/z 431 (M + H$^+$). To a solution of the above amide-oxime intermediate (70.0 mg, 0.16 mmol) in 1,2-dichloroethane (2.0 mL) at 23 °C was added trimethyl orthoformate (51.6 mg, 0.48 mmol), followed by boron trifluoride diethyl etherate (3.40 mg, 0.02 mmol). The reaction mixture was stirred at 70 °C and stirred for 12 h. The solvent was removed in vacuo, and the resulting crude product was purified by flash column chromatography using a 20→60% gradient of ethyl acetate/heptane to afford 68.0 mg (95% yield) of **22** as a colorless solid. ^{1}H NMR (400 MHz, MeOD) δ 9.15 (s, 1H), 7.91−7.85 (m, 2H), 7.62−7.57 (m, 2H), 4.42 (dd, J = 8.30, 6.35 Hz, 1H), 3.88 (ddd, J = 15.4, 9.37, 6.05 Hz, 1H), 3.72−3.61 (m, 1H), 3.29−3.22 (m, 1H), 3.18−3.07 (m, 1H), 2.22−2.00 (m, 3H), 1.77−1.63 (m, 1H). LCMS m/z 441 (M + H$^+$).

*(R)-2-{N-[3-(1,2,4-Oxadiazol-3-yl)propyl]-4-chlorophenylsulfonamido}-5,5,5-trifluoropentanamide (**23**).* To a solution of **11** (100 mg, 0.24 mmol) in ethanol (1.5 mL) at 23 °C was added hydroxylamine·HCl (34.5 mg, 0.49 mmol), followed by triethylamine (0.05 mL, 0.36 mmol). The reaction mixture was stirred at 80 °C for 16 h, after which time the solvent was removed in vacuo. To this crude product was added pyridine (1.50 mL, 19.0 mmol), followed by trimethyl orthoformate (2.00 mL, 18.3 mmol) and boron trifluoride diethyl etherate (3.40 mg, 0.024 mmol). The reaction mixture was stirred at 80 °C for 16 h. The solvent was removed in vacuo, and the crude product was purified by preparative reversed phase HPLC (Phenomenex Gemini C18 column; mobile phase: 95/5→5/95 gradient of 0.1% NH_4OH in water/0.1% NH_4OH in methanol) to afford 15.0 mg (15% yield) of **23** as a clear gum. ^{1}H NMR (400 MHz, $CDCl_3$) δ 8.62 (s, 1H), 7.74−7.72 (m, 2H), 7.59−7.52 (m, 2H), 6.52 (br s, 1H), 5.49 (br s, 1H), 4.24 (dd, J = 8.40, 6.64 Hz, 1H), 3.49−3.36 (m, 1H), 3.23 (ddd, J = 14.8, 9.81, 4.88 Hz, 1H), 2.80 (t, J = 7.22 Hz, 2H), 2.23−1.69 (m, 4H), 1.43−1.28 (m, 2H). LCMS m/z 456 (M + H$^+$).

*(R)-2-{N-{[1-(1,2,4-Oxadiazol-3-yl)cyclopropyl]methyl}-4-chlorophenylsulfonamido}-5,5,5-trifluoropentanamide (**24**).* Compound **19** (50.0 mg, 0.12 mmol), hydroxylamine (50 wt % in water, 32.3 mg, 0.49 mmol), trimethyl orthoformate (23.9 mg, 0.23 mmol), trifluoride diethyl etherate (2.10 mg, 0.015 mmol), and boron trifluoride diethyl etherate (2.10 mg, 0.015 mmol) were used to synthesize **24** using the procedure described for the preparation of **3**. The crude product was purified by flash column chromatography using a 0→80% gradient of ethyl acetate/heptane to afford 22.0 mg of **24** and **19** as a 9:1 mixture. This material was repurified by preparative HPLC (Princeton 2-Ethyl Pyridine column; mobile phase: 95/5 → 5/95 gradient of heptane/ethanol) to afford 3.00 mg (8.6% yield) of **24** as a white solid. ^{1}H NMR (500 MHz, $CDCl_3$) δ 8.54 (s, 1H), 7.87−7.69 (m, 2H), 7.57−7.45 (m, 2H), 6.96 (br s, 1H), 5.36 (br s, 1H), 4.30 (dd, J = 9.03, 5.86 Hz, 1H), 3.82−3.69 (m, 2H), 2.44−2.35 (m, 1H), 2.17−2.03 (m, 1H), 1.91−1.79 (m, 1H), 1.55−1.47 (m, 1H), 1.44 (ddd, J = 9.33, 7.02, 4.64 Hz, 1H), 1.34−1.23 (m, 3H). LCMS m/z 467 (M + H$^+$).

*(R)-2-{N-{[(1S,3S)-3-(1,2,4-Oxadiazol-3-yl)cyclobutyl]methyl}-4-chlorophenylsulfonamido}-5,5,5-trifluoropentanamide (**25**).* To a solution of **15** (120 mg, 0.27 mmol) in ethanol (2.5 mL) at 23 °C was added hydroxylamine·HCl (19.4 mg, 0.27 mmol), followed by potassium carbonate (18.9 mg, 0.14 mmol). The reaction mixture was stirred at 80 °C for 48 h. Ethyl acetate (10 mL) was then added at 23 °C, the mixture was filtered, and the filtrate was concentrated in vacuo. To this crude product in tetrahydrofuran (1.0 mL) was added trimethyl orthoformate (1.50 mL, 14.0 mmol) and boron trifluoride diethyl etherate (1.40 μL, 0.05 mmol). The reaction mixture was stirred at 80 °C for 48 h. The solvent was removed in vacuo, and the crude product was purified by preparative HPLC (Phenomenex Phenyl Hexyl column; mobile phase: 95:5 → 0:100 gradient of 0.1% formic acid in water/0.1% formic acid in methanol) to afford 1.60 mg (2.5% yield) of **25** as a pale-white solid. ^{1}H NMR (400 MHz, MeOD) δ 9.10−9.07 (m, 1H), 7.87−7.86 (m, 2H), 7.61−7.55 (m, 2H), 4.36 (t, J = 8.00 Hz, 1H), 3.56−3.45 (m, 2H), 2.77−2.65 (m, 1H), 2.48−2.38 (m, 2H), 2.12−1.94 (m, 6H), 1.61−1.49 (m, 1H). LCMS m/z 503 (M + Na).

*3-(Hydroxymethyl)-1-methylcyclobutanecarbonitrile (**26**).* To a solution of 3-methylenecyclobutanecarbonitrile (**27**, 1.00 g, 9.33 mmol) in tetrahydrofuran (40 mL) at 0 °C was added a solution of 9-borabicyclo[3.3.1]nonane (0.50 M in THF, 26.1 mL, 13.1 mmol) dropwise over a period of 10 min. The reaction mixture was stirred warmed to room temperature and stirred at that temperature for 2 h. Water (50 mL) and sodium borate (4.30 g, 11.3 mmol) were then

added, and the resulting mixture was stirred at room temperature for 12 h. The mixture was then filtered, and the filtrant was washed with diethyl ether (20 mL). The layers of the filtrate were separated, and the organic layer was extracted with diethyl ether (2 × 20 mL). The combined organic extracts were washed with brine (50 mL), dried ($MgSO_4$), and filtered. The solvent was removed in vacuo, and the crude product was purified by flash column chromatography using a 25 → 50% gradient of ethyl acetate/heptane to afford 192 mg (53% yield) of **26** (as a 2:1 ratio of *cis*- and *trans*-isomers). ^{1}H NMR (400 MHz, $CDCl_3$) δ 3.70−3.54 (m, 2H), 2.81−2.33 (m, 3H), 2.16−1.87 (m, 2H), 1.60−1.40 (m, 3H). APCI m/z 126 (M + H).

■ ASSOCIATED CONTENT

Supporting Information

Synthesis of compound **4**, ^{1}H and ^{13}C NMR spectra of compound **3**, X-ray crystallography data for compounds **1** and **3**, and biology protocols. This material is available free of charge via the Internet at http://pubs.acs.org.

■ AUTHOR INFORMATION

Corresponding Author

*Phone: (860) 686-3247. E-mail: Antonia.Stepan@pfizer.com.

Notes

The authors declare no competing financial interest.

■ ACKNOWLEDGMENTS

We thank Drs. Amit S. Kalgutkar, Anabella Villalobos, and Joshua R. Dunetz for helpful suggestions in preparing this article, Drs. Anthony Kreft, David Rotella, and Alexander Porte for fruitful discussions during the project transition from Wyeth, and Brian Samas and Ivan Samardjiev for the single crystal X-ray structure elucidation of compounds **1** and **3**. We also thank James Bradow, Robert P. Depianta, and Drs. Qi Yan and Laurence Philippe-Venec from the purification group and Brendon Kapinos, Walter E. Mitchell, Jillian B. Van Hausen, James J. Frederico, III, John P. Umland, Mark W. Snyder, and Dr. Marina Y. Shalaeva from the ADME high-throughput screening group at Pfizer, Groton.

■ ABBREVIATIONS USED

AD, Alzheimer's disease; Aβ, amyloid-β; APP, β-amyloid precursor protein; BA, brain availability; B/P, brain to plasma ratio; $CL_{int,app}$, apparent intrinsic clearance; CNS MPO, central nervous system multiparameter optimization; CSF, cerebrospinal fluid; CYP, cytochrome P450; f_u, fraction unbound; GSI, γ-secretase inhibitor; HHEP, human hepatocytes; HLM, human liver microsomes; iv, intravenous; MDCK, Madine Darby canine kidney; MDR1, multidrug resistance protein (p-glycoprotein); PD, pharmacodynamics; PK, pharmacokinetic; po (per os), oral administration; SAR, structure−activity relationship

■ REFERENCES

(1) Selkoe, D. J. Alzheimer's disease. *Cold Spring Harbor Perspect. Biol.* **2011**, 3, doi: 10.1101/cshperspect.a004457.

(2) Hardy, J.; Selkoe, D. J. The amyloid hypothesis of Alzheimer's disease: progress and problems on the road to therapeutics. *Science* **2002**, *297*, 353−356.

(3) (a) Sinha, S.; Liberburg, I. Cellular mechanisms of β-amyloid production and secretion. *Proc. Natl. Acad. Sci. U.S.A.* **1999**, *96*, 11049−11053. (b) Bergmans, B. A.; De Strooper, B. γ-secretases: from cell biology to therapeutic strategies. *Lancet Neurol.* **2010**, *9*, 215−226. (c) Wolfe, M. S. The γ-secretase complex: membrane-embedded proteolytic ensemble. *Biochemistry* **2006**, *45*, 7931−7939.

(4) Pettersson, M.; Kauffman, G. W.; am Ende, C. W.; Patel, N. C.; Stiff, C.; Tran, T. P.; Johnson, D. S. Novel γ-secretase modulators: a review of patents from 2008 to 2010. *Expert Opin. Ther. Pat.* **2011**, *21*, 205−226.

(5) (a) Kopan, R; Ilagan, M. X. γ-Secretase: proteasome of the membrane? *Nature Rev. Mol. Cell. Biol.* **2004**, *5*, 499−504. (b) Beel, A. J.; Sanders, C. R. Substrate specificity of gamma-secretase and other intramembrane proteases. *Cell. Mol. Life Sci.* **2008**, *65*, 1311−1334.

(6) For reviews see: (a) Kreft, A. F.; Martone, R.; Porte, A. Recent advances in the identification of γ-secretase inhibitors to clinically test the Aβ oligomer hypothesis of Alzheimer's disease. *J. Med. Chem.* **2009**, *52*, 6169−6188. (b) Olson, R. E.; Albright, C. F. Recent Progress in the Medicinal Chemistry of γ-Secretase Inhibitors. *Curr. Top. Med. Chem.* **2008**, *8*, 17−33.

(7) Gillman, K. W.; Starrett, J. E.; Parker, M. F.; Xie, K.; Bronson, J. J.; Marcin, L. R.; McElhone, K. E.; Bergstrom, C. P.; Mate, R. A.; Williams, R.; Meredith, J. E.; Burton, C. R.; Barten, D. M.; Toyn, J. H.; Roberts, S. B.; Lentz, K. A.; Houston, J. G.; Zaczek, R.; Albright, C. F.; Decicco, C. P.; Macor, J. E.; Olson, R. E. Discovery and Evaluation of BMS-708163, a Potent, Selective and Orally Bioavailable γ-Secretase Inhibitor. *ACS Med. Chem. Lett.* **2010**, *1*, 120−124.

(8) (a) Brodney, M. A.; Auperin, D. D.; Becker, S. L.; Bronk, B. S.; Brown, T. M.; Coffman, K. J.; Finley, J. E.; Hicks, C. D.; Karmilowicz, M. J.; Lanz, T. A.; Liston, D.; Liu, X.; Martin, B.-A.; Nelson, R. B.; Nolan, C. E.; Oborski, C. E.; Parker, C. P.; Richter, K. E. G.; Pozdnyakov, N.; Sahagan, B. G.; Schachter, J. B.; Sokolowski, S. A.; Tate, B.; Van Deusen, J. W.; Wood, D. E.; Wood, K. M. Diamide amino-imidazoles: a novel series of γ-secretase inhibitors for the treatment of Alzheimer's disease. *Bioorg. Med. Chem. Lett.* **2011**, *21*, 2631−2636. (b) Brodney, M. A.; Auperin, D. D.; Becker, S. L.; Bronk, B. S.; Brown, T. M.; Coffman, K. J.; Finley, J. E.; Hicks, C. D.; Karmilowicz, M. J.; Lanz, T. A.; Liston, D.; Liu, X.; Martin, B.-A.; Nelson, R. B.; Nolan, C. E.; Oborski, C. E.; Parker, C. P.; Richter, K. E. G.; Pozdnyakov, N.; Sahagan, B. G.; Schachter, J. B.; Sokolowski, S. A.; Tate, B.; Wood, D. E.; Wood, K. M.; Van Deusen, J. W.; Zhang, L. Design, synthesis, and in vivo characterization of a novel series of tetralin amino imidazoles as γ-secretase inhibitors: discovery of PF-3084014. *Bioorg. Med. Chem. Lett.* **2011**, *21*, 2637−2640.

(9) Stepan, A. F.; Karki, K.; McDonald, W. S.; Dorff, P. H.; Dutra, J. K.; DiRico, K. J.; Won, A.; Subramanyam, C.; Efremov, I. V.; O'Donnell, C. J.; Nolan, C. E.; Becker, S. L.; Pustilnik, L. R.; Sneed, B.; Sun, H.; Lu, Y.; Robshaw, A. E.; Riddell, D.; O'Sullivan, T. J.; Sibley, E.; Capetta, S.; Atchison, K.; Hallgren, A. J.; Miller, E.; Wood, A.; Obach, R. S. *J. Med. Chem.* **2011**, *54*, 7772−7783.

(10) Lovering, F.; Bikker, J.; Humblet, C. Escape from Flatland: Increasing Saturation as an Approach to Improving Clinical Success. *J. Med. Chem.* **2009**, *52*, 6752−6756.

(11) (a) Pellicciari, R.; Raimondo, M.; Marinozzi, M.; Natalini, B.; Costantino, G; Thomsen, C. (*S*)-(+)-2-(3′-Carboxybicyclo[1.1.1]-pentyl)-glycine, a structurally new group 1 metabotropic glutamate receptor antagonist. *J. Med. Chem.* **1996**, *39*, 2874−2876. (b) Costantino, G.; Maltoni, K.; Marinozzi, M.; Camaioni, E.; Prezeau, L.; Pin, J.-P.; Pellicciari, R. Synthesis and biological evaluation of 2-(3′-(1*H*-tetrazol-5-yl)bicyclo[1.1.1]pent-1-yl)glycine (S-TBPG), a novel mGlu1 receptor antagonist. *Bioorg. Med. Chem.* **2001**, *9*, 221−227.

(12) Della, E. W.; Taylor, D. K. Synthesis of Some Bridgehead−Bridgehead-Disubstituted Bicyclo[1.1.1]pentanes. *J. Org. Chem.* **1994**, *59*, 2986−2996.

(13) (a) Parker, M. F.; McElhone, K. E.; Mate, R. A.; Bronson, J. J.; Gai, Y.; Bergstrom, C. P.; Marcin, L. R.; Macor, J. E. Preparation of α-(*N*-sulfonamido)acetamides as β-amyloid inhibitors. PCT Int. Appl. WO 2003053912, A1 20030703, CAN 139:85645, AN 2003:511281, 2003; (b) Starrett, J. E.; Gillman, K. W.; Olson, R. E. A novel alpha-(*n*-sulfonamido)acetamide compound as an inhibitor of beta amyloid peptide production. PCT Int. Appl. WO 2010107435, A1 20100923, 2010.

(14) Callegari, E.; Malhotra, B.; Bungay, P. J.; Webster, R.; Fenner, K. S.; Kempshall, S.; Laperle, J. L.; Michel, M. C.; Kay, G. G. A comprehensive nonclinical evaluation of the CNS penetration potential of

antimuscarinic agents for the treatment of overactive bladder. *Br. J. Clin. Pharmacol.* **2011**, *72*, 235−246.
(15) Hosea, N. A.; Collard, W. T.; Cole, S.; Maurer, T. S.; Fang, R. X.; Jones, H.; Kakar, S. M.; Nakai, Y.; Smith, B. J.; Webster, R.; Beaumont, K. Prediction of human pharmacokinetics from preclinical information: comparative accuracy of quantitative prediction approaches. *J. Clin. Pharmacol.* **2009**, *49*, 513−533.
(16) Lombardo, F.; Shalaeva, M. Y.; Tupper, K. A.; Gao, F. ElogD(oct): a tool for lipophilicity determination in drug discovery. 2. Basic and neutral compounds. *J. Med. Chem.* **2001**, *44*, 2490−2497.
(17) Ritchie, T. J.; Macdonald, S. J. F. The impact of aromatic ring count on compound developability: Are too many aromatic rings a liability in drug design? *Drug Discovery Today* **2009**, *14*, 1011−1020.
(18) Edwards, M. P.; Price, D. A. Role of physicochemical properties and ligand lipophilicity efficiency in addressing drug safety risks. *Annu. Rep. Med. Chem.* **2010**, *45*, 381−391.
(19) (a) Wager, T. T.; Chandrasekaran, R. Y.; Hou, X.; Troutman, M. D.; Verhoest, P. R.; Villalobos, A.; Will, Y. Defining desirable central nervous system drug space through the alignment of molecular properties, in vitro ADME, and safety attributes. *ACS Chem. Neurosci.* **2010**, *1*, 420−434. (b) Wager, T. T.; Hou, X.; Verhoest, P. R.; Villalobos, A. Moving beyond rules: the development of a central nervous system multiparameter optimization (CNS MPO) approach to enable alignment of druglike properties. *ACS Chem. Neurosci.* **2010**, *1*, 435−449.
(20) Zientek, M.; Miller, H.; Smith, D.; Dunklee, M. B.; Heinle, L.; Thurston, A.; Lee, C.; Hyland, R.; Fahmi, O.; Burdette, D. Development of an in vitro drug−drug interaction assay to simultaneously monitor five cytochrome P450 isoforms and performance assessment using drug library compounds. *J. Pharmacol. Toxicol. Methods.* **2008**, *58*, 206−214.
(21) Finlayson, K.; Witchel, H. J.; McCulloch, J.; Sharkey, J. Acquired QT interval prolongation and HERG: implications for drug discovery and development. *Eur. J. Pharmacol.* **2004**, *500*, 129−142.
(22) Kalgutkar, A. S.; Vaz, A. D.; Lame, M. E.; Henne, K. R.; Soglia, J.; Zhao, S. X.; Abramov, Y. A.; Lombardo, F.; Collin, C.; Hendsch, Z. S.; Hop, C. E. Bioactivation of the nontricyclic antidepressant nefazodone to a reactive quinone-imine species in human liver microsomes and recombinant cytochrome P4503A4. *Drug Metab. Dispos.* **2005**, *33*, 243−253.
(23) (a) Patani, G. A.; LaVoie, E. J. Bioisosterism: A Rational Approach in Drug Design. *Chem. Rev.* **1996**, *96*, 3147−3176. (b) Meanwell, N. A. Synopsis of Some Recent Tactical Application of Bioisosteres in Drug Design. *J. Med. Chem.* **2011**, *54*, 2529−2591.
(24) Lu, Y.; Zhang, L.; Nolan, C. E.; Becker, S. L.; Atchison, K.; Robshaw, A. E.; Pustilnik, L. R.; Osgood, S. M.; Miller, E. H.; Stepan, A. F.; Subramanyam, C.; Efremov, I.; Hallgren, A. J.; Riddell, D. Quantitative Pharmacokinetic/Pharmacodynamic Analyses Suggest That 129/SVE Mouse Is A Suitable Preclinical Pharmacology Model For Identifying Small Molecule Gamma Secretase Inhibitors. *J. Pharmacol. Exp. Ther.* **2011**, *339*, 922−934.
(25) Burton, C. R.; Meredith, J. E.; Barten, D. M.; Goldstein, M. E.; Krause, C. M.; Kieras, C. J.; Sisk, L.; Iben, L. G.; Polson, C.; Thompson, M. W.; Lin, X.-A.; Corsa, J.; Fiedler, T.; Pierdomenico, M.; Cao, Y.; Roach, A. H.; Cantone, J. L.; Ford, M. J.; Drexler, D. M.; Olson, R. E.; Yang, M. G.; Bergstron, C. P.; McElhone, K. E.; Bronson, J. J.; Macor, J. E.; Blat, Y.; Grafstrom, R. H.; Stern, A. M.; Seiffert, D. A.; Zaczek, R.; Albright, C. F.; Toyn, J. H. The amyloid-β rise and γ-secretase inhibitor potency depend on the level of substrate expression. *J. Biol. Chem.* **2008**, *283*, 22992−23003.
(26) Lanz, T. A.; Wood, K. M.; Richter, K. E.; Nolan, C. E.; Becker, S. L.; Pozdnyakov, N.; Martin, B. A.; Du, P.; Oborski, C. E.; Wood, D. E.; Brown, T. M.; Finley, J. E.; Sokolowski, S. A.; Hicks, C. D.; Coffman, K. J.; Geoghegan, K. F.; Brodney, M. A.; Liston, D.; Tate, B. Pharmacodynamics and pharmacokinetics of the γ-secretase inhibitor PF-3084014. *J. Pharmacol. Exp. Ther.* **2010**, *334*, 269−277.